

Theory and Observations of Runaway Electrons in the Solar Wind

Kosta Horaites

Collaborators: S. Boldyrev, M. V. Medvedev, P. Astfalk,
F. Jenko, L. B. Wilson III, A. F. Viñas, J. Merka,
S. I. Krasheninnikov, C. Salem, S. D. Bale, M. Pulupa

ESAC Madrid, 5/28/2019



art: Beth Racette

Kinetic Theory and Observations of Runaway Electrons in the Solar Wind

Introduction

Kinetic Strahl Model

Observations: SWE Strahl Detector

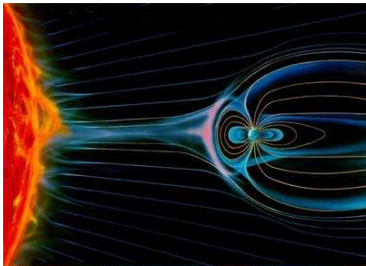
Stability Analysis

Conclusions

Solar Wind



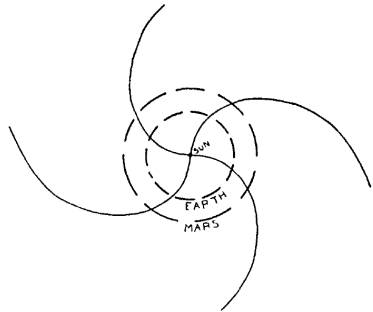
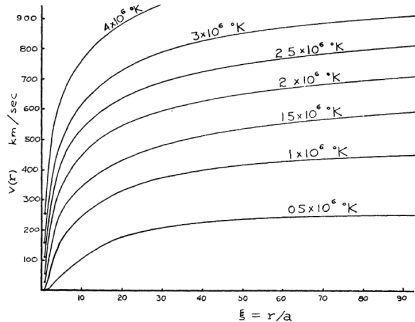
© 1998 Andreas Oaida



Solar wind, as depicted in this artist's illustration, travels from the Sun and envelopes the Earth's magnetic field. High-energy pulses of solar wind from sunspot activity ("solar bursts" or "plasma bubbles") travel from the Sun to the Earth at speeds exceeding 500 miles per second. The pulses distort the Earth's magnetic field and produce geomagnetic storms that disrupt the Earth's environment.



The Parker Spiral (Parker, 1958)

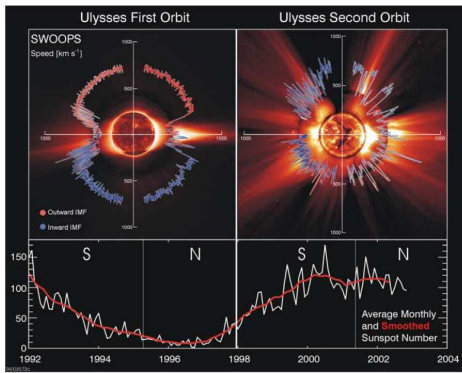


The constant outward solar wind flow, with the sun's rotation, twists the **B**-field into a spiral pattern.

Fast and Slow solar wind

- ▶ Fast wind: $v_{sw} \gtrsim 650$ km/sec
 - ▶ low n
 - ▶ high T
 - ▶ originates from coronal holes
 - ▶ typically seen near poles

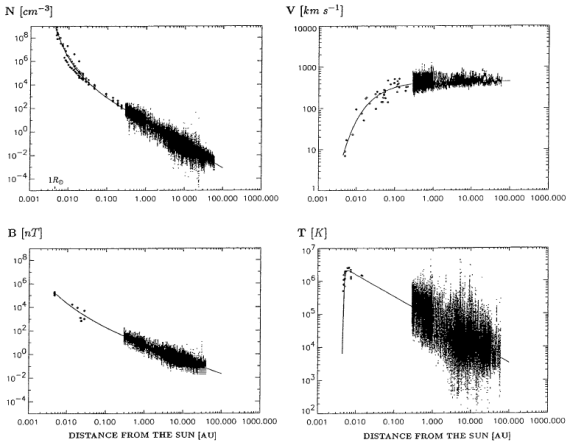
- ▶ Slow wind: $v_{sw} \sim 400$ km/sec
 - ▶ high n
 - ▶ low T
 - ▶ originates from active regions
 - ▶ typically seen in ecliptic



McComas et al., 2003

In this talk we will focus on the **fast** wind that is sometimes observed in the **ecliptic**.

Plasma Parameters vs. Distance (protons)



► $n \sim r^{-2}$

► $v_{sw} \sim \text{const.}$

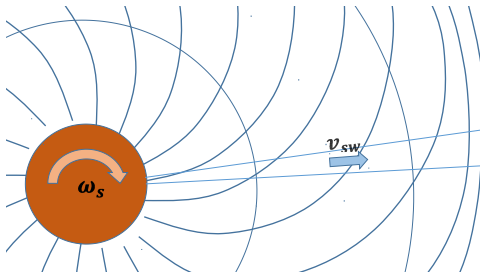
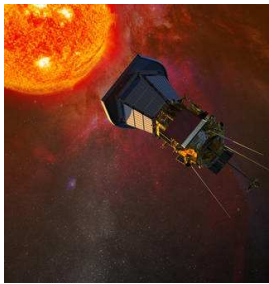
► $T \sim r^{-2/3}$

Köhlein, 1996

We expect heat to flow *within* the solar wind, from hot regions to cool regions.

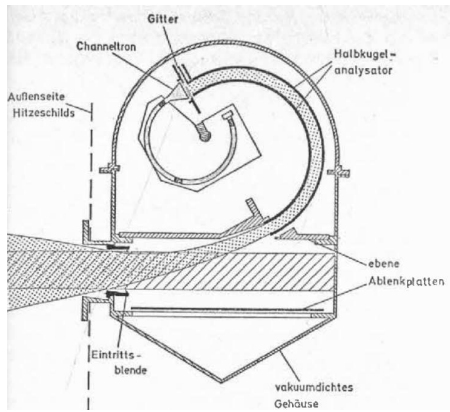
Electron Distribution: Kinetic Physics

Question: What does the electron distribution function $f(\mathbf{v})$ look like in detail?



Source: JHU/APL

Measuring $f(v)$: Electrostatic Analyzers



Schwenn et al., 1975



<https://solarsystem.nasa.gov/>

- ▶ Concentric circular electrodes, radii $\approx R$
- ▶ Circular path $mv^2/R = eE \rightarrow mv^2/2 = eER/2$

Suprathermal electron populations

$$f(v_{\perp}, v_{\parallel}) = f_c + f_h + f_s$$

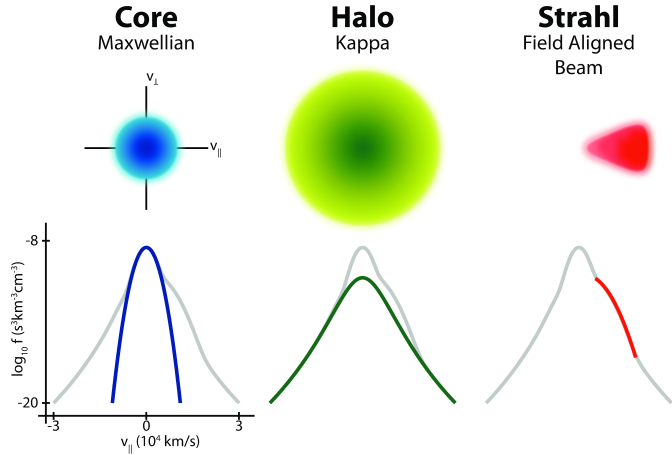


Illustration: M. Pulupa

Heat carried by electrons appears as a field-parallel skewness in the distribution function.

Thermal conductivity in the solar wind

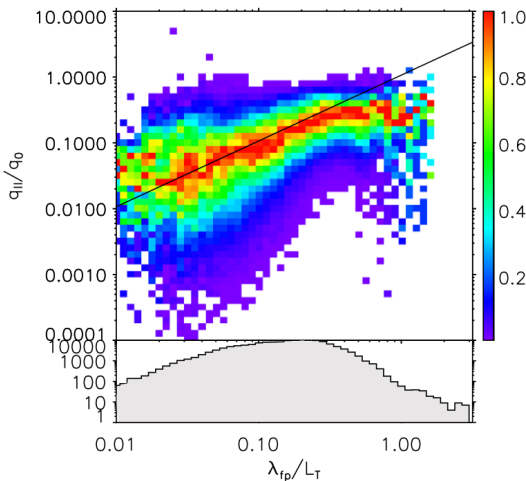
Heat flux \mathbf{q} :

$$\mathbf{q} \equiv \frac{m_e}{2} \int \mathbf{v} v^2 f(\mathbf{v}) d^3 v$$
$$[\mathbf{q}] = \frac{W}{m^2}$$

Knudsen number γ :

$$\gamma = \lambda_{mfp} \frac{d \ln T}{dx} = \frac{\lambda_{mfp}}{L_T}$$

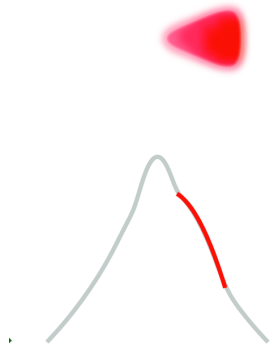
- ▶ $\gamma \ll 1$: $\mathbf{q} = -\kappa \nabla T$
(collisional)
- ▶ $\gamma \gg 1$: $q \sim n T v_{th}$
(collisionless)



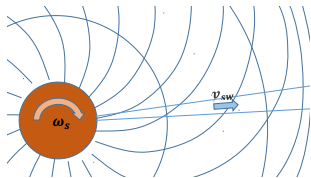
Wind data, $r=1$ AU (Bale et al., 2013)

Strahl: Intuitive Explanation

Strahl
Field Aligned
Beam



- ▶ Electrons focus into a beam along \mathbf{B} , as they try to conserve their magnetic moment ($\frac{v_\perp^2}{B}$)



- ▶ But, angular diffusion (provided, e.g., by Coulomb collisions with other particles) broadens the distribution somewhat.

Kinetic Theory and Observations of Runaway Electrons in the Solar Wind

Introduction

Kinetic Strahl Model

Observations: SWE Strahl Detector

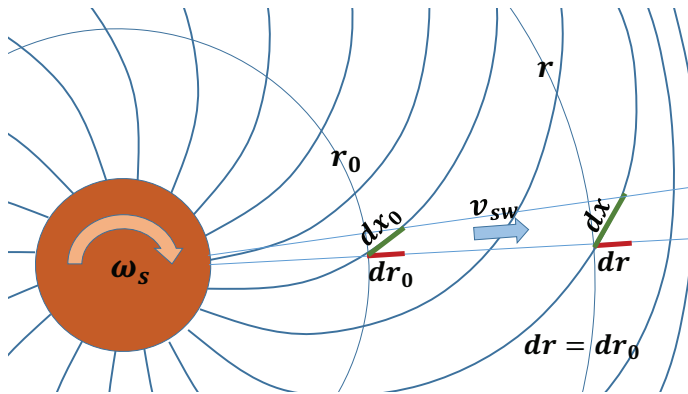
Stability Analysis

Conclusions

Kinetic Theory (Horaites et al., 2019)

Drift Kinetic Equation for $f(x, M, v_{\parallel})$, assuming $|\mathbf{v}| \gg v_{sw}$:

$$v_{\parallel} \hat{b} \cdot \nabla f + \left(\frac{MB(x)}{2} \nabla \cdot \hat{b} - \frac{q_e(d\phi/dx)}{m_e} \right) \frac{\partial f}{\partial v_{\parallel}} = \hat{C}(f)$$



Kinetic Theory (Horaites et al., 2019)

Drift Kinetic Equation for $f(x, M, v_{\parallel})$, assuming $|\mathbf{v}| \gg v_{sw}$:

$$v_{\parallel} \hat{b} \cdot \nabla f + \left(\frac{MB(x)}{2} \nabla \cdot \hat{b} - \frac{q_e(d\phi/dx)}{m_e} \right) \frac{\partial f}{\partial v_{\parallel}} = \hat{C}(f)$$

Change variables—distance $y \propto r$ (flux freezing),
electron energy E , and magnetic moment M :

$$dy \equiv \left(\frac{16\pi e^4 \Lambda}{m_e^2 E} \right) \left(\frac{n(x)}{B(x)} \right) dx, \quad E \equiv v^2 + (2/m_e) q_e \phi(x), \quad M \equiv v_{\perp}^2 / B(x)$$

Kinetic Theory (Horaites et al., 2019)

Drift Kinetic Equation for $f(x, M, v_{\parallel})$, assuming $|\mathbf{v}| \gg v_{sw}$:

$$v_{\parallel} \hat{b} \cdot \nabla f + \left(\frac{MB(x)}{2} \nabla \cdot \hat{b} - \frac{q_e(d\phi/dx)}{m_e} \right) \frac{\partial f}{\partial v_{\parallel}} = \hat{C}(f)$$

Change variables—distance $y \propto r$ (flux freezing),
electron energy E , and magnetic moment M :

$$dy \equiv \left(\frac{16\pi e^4 \Lambda}{m_e^2 E} \right) \left(\frac{n(x)}{B(x)} \right) dx, \quad E \equiv v^2 + (2/m_e) q_e \phi(x), \quad M \equiv v_{\perp}^2 / B(x)$$

Strahl regime: assume large energies ($E \approx v^2$) and small angles ($\frac{MB}{E} \ll 1$). DKE then reduces to a simple form:

$$\frac{\partial}{\partial y} f(y, E, M) = \frac{\partial}{\partial M} M \frac{\partial}{\partial M} f$$

Strahl Solution

$$\frac{\partial}{\partial y} f(y, E, M) = \frac{\partial}{\partial M} M \frac{\partial}{\partial M} f$$

Solution (2D diffusion):

$$f(y, E, M) = \frac{C(E)}{y} \exp\left(-\frac{M}{y}\right)$$

Assume Parker spiral model (in the ecliptic):

$$B(r) = \frac{B(r_{45})}{\sqrt{2}} \frac{r_{45}}{r} \sqrt{1 + \frac{r_{45}^2}{r^2}},$$

where $r_{45} \approx 1$ AU. Cast f in terms of r , v , and $\mu = v_{\parallel}/v$:

$$f(r, \mu, v) = \frac{C(v^2)}{r} \exp\left\{-\frac{v^4(1 - \mu^2)}{\sqrt{1 + r_{45}^2/r^2}} \left(\frac{m_e^2}{16\pi n_{45} r_{45} e^4 \Lambda}\right)\right\}$$

Angular FWHM of Strahl

Recalling $\mu = \cos \theta$, and approximating $\sin \theta \approx \theta$, we see strahl has Gaussian angular dependence:

$$f(\theta) \propto \exp\{-A(r, r_{45})n^{-1}K^2\theta^2\},$$

$$\text{where } K \equiv \frac{m_e v^2}{2}.$$

The full width at half maximum, (θ_{FWHM}), is given by the formula:

$$\theta_{FWHM} \approx 24^\circ \left(\frac{K}{100 \text{ eV}} \right)^{-1} \left(\frac{n(r_{45})}{5 \text{ cm}^{-3}} \right)^{1/2} \left(1 + \frac{r_{45}^2}{r^2} \right)^{1/4}, \quad (1)$$

Note the scaling relations:

- i For given n , $\theta_{FWHM} \propto K^{-1}$
- ii For given K , $\theta_{FWHM} \propto \sqrt{n}$

Narrow strahl predicted! Need high angular resolution to detect it.

Kinetic Theory and Observations of Runaway Electrons in the Solar Wind

Introduction

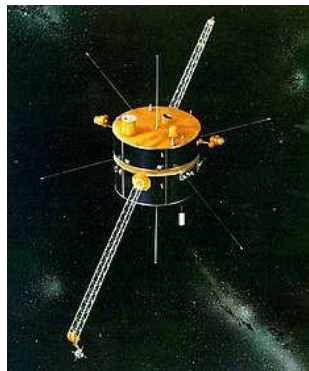
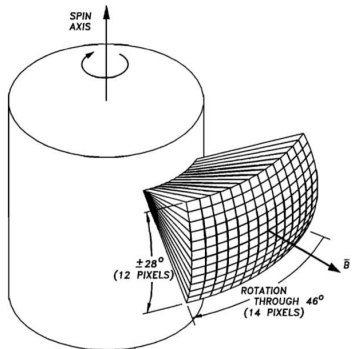
Kinetic Strahl Model

Observations: SWE Strahl Detector

Stability Analysis

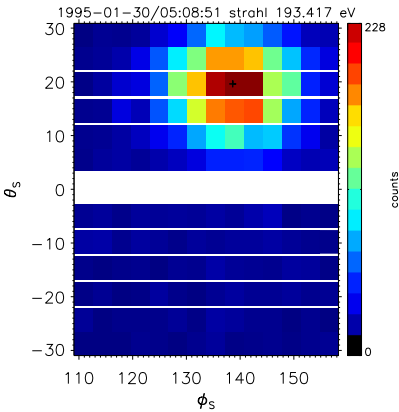
Conclusions

SWE Strahl Detector

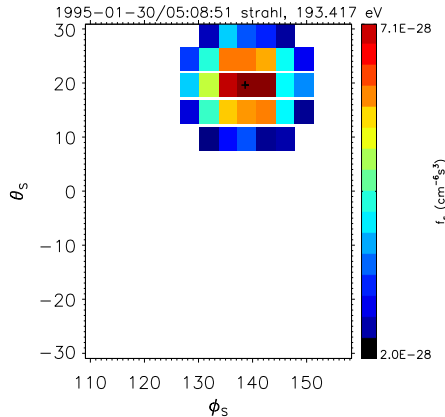


- ▶ Left: SWE strahl field of view
(Ogilvie, 2000)
- ▶ Top right: SWE strahl detector
(<http://web.mit.edu>)
- ▶ Bottom right: Wind spacecraft 1 AU
(<https://wind.nasa.gov>)

SWE Strahl Detector



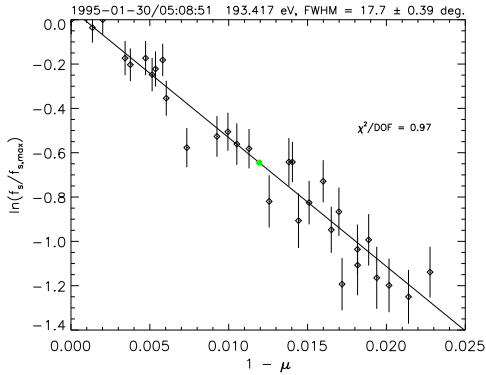
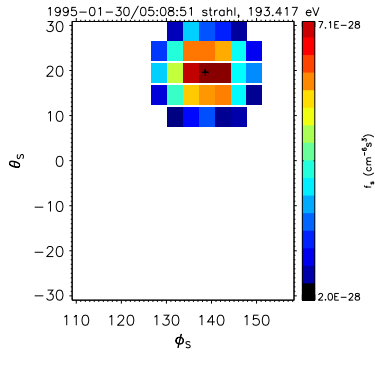
Raw counts



Cleaned distribution f (Horaites et al., 2018a)

Strahl electron counts measured at 3.5x4.5 degree resolution

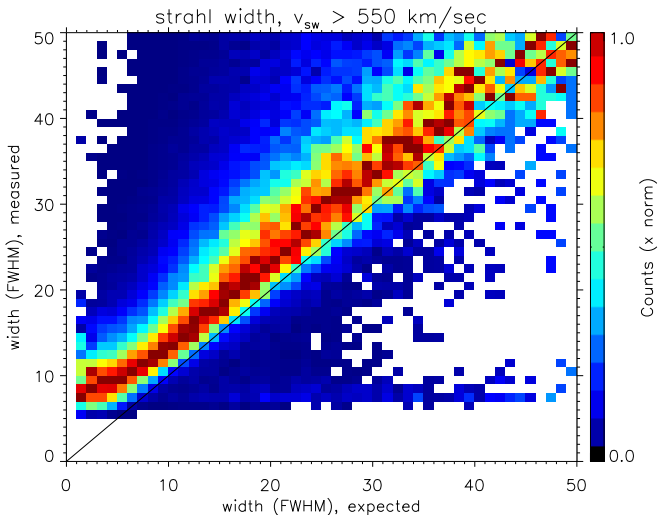
Least squares: strahl width (Horaites et al., 2018a)



$$\text{Model: } \ln \left\{ \frac{f(\mu)}{f_{\max}} \right\} \propto (1 - \mu)$$

Fit yields a “Measured θ_{FWHM} ” (green dot).

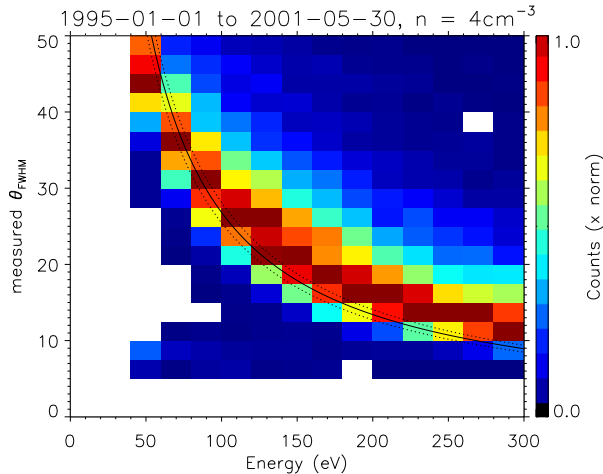
Model/Data Comparison: $v_{sw} > 550$ km/s



Model/Data Comparison:

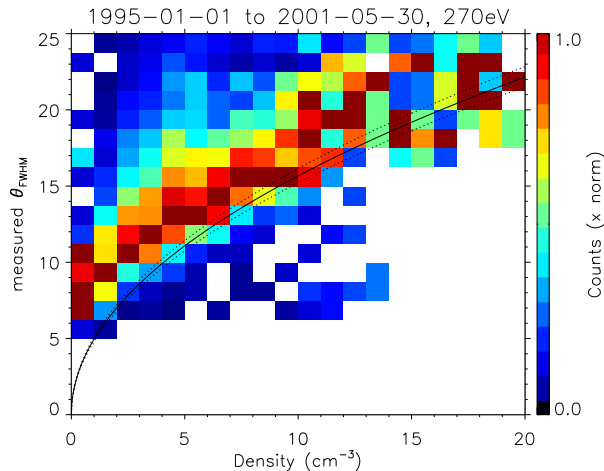
$v_{sw} > 550 \text{ km/s}$, $3.5 < n < 4.5 \text{ cm}^{-3}$

i For given n , $\theta_{FWHM} \propto K^{-1}$



Model/Data Comparison: $v_{sw} > 550$ km/s, $K = 271$ eV

ii For given K , $\theta_{FWHM} \propto \sqrt{n}$



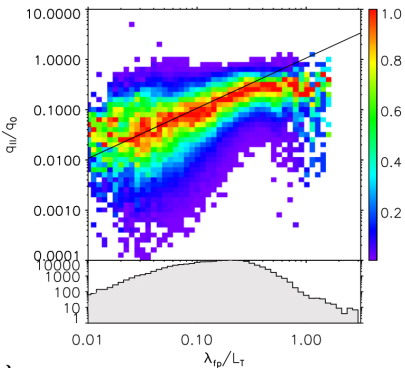
Horaites et al., 2018a

Measuring energy dependence: F_{ave}

$$f(r, \mu, v) = \frac{C(v^2)}{r} \exp \left\{ -\frac{v^4(1-\mu^2)}{\sqrt{1+r_{45}^2/r^2}} \left(\frac{m_e^2}{16\pi n_{45} r_{45} e^4 \Lambda} \right) \right\}$$

- ▶ Want to measure the function $C(v^2)$.
- ▶ But, $f(\mathbf{v})$ measured by SWE/strahl 1 energy at a time.
- ▶ Consider also that \mathbf{q} , and by extension the strahl, depends on collisionality ($\tilde{\gamma}$).

Approach: construct *averaged* distribution F_{ave} from all the strahl data, sorted by $\tilde{\gamma}$.



$$\tilde{\gamma} \equiv \frac{T^2}{2\pi e^4 \Lambda n r} \sim \frac{\lambda_{mfp}}{L_T}$$

Bale et al., 2013

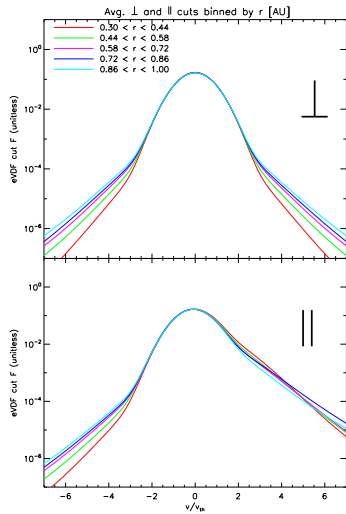
Normalized distribution function $F(\mathbf{v}/v_{th})$

- ▶ $F(\mathbf{v}/v_{th})$ is a normalized, dimensionless function that characterizes the “shape” of the distribution function $f(\mathbf{v})$.
- ▶ Introduced by Krasheninnikov (1988) in theoretical context of self-similar distributions.

$$F(\mathbf{v}/v_{th}) \equiv \frac{v_{th}^3 f(\mathbf{v})}{n}$$

Normalization:

$$\int f(\mathbf{v}) d^3v = n, \quad \int F d^3(v/v_{th}) = 1$$



Helios F , $0.3 < r < 1$ AU
(unpublished)

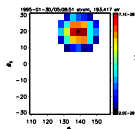
Asymptotic strahl solutions (high-energy, field-parallel)

Model distribution can be written as:

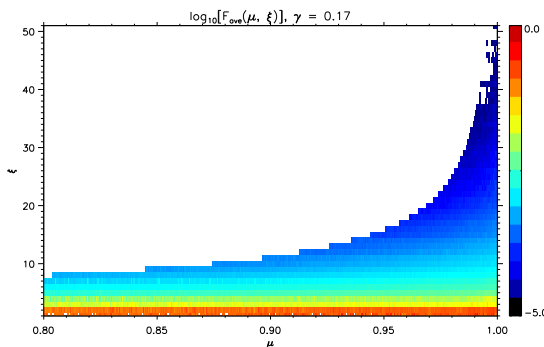
$$F(\mu, v/v_{th}) = C_0 \left(\frac{v}{v_{th}} \right)^{2\epsilon} \exp \left\{ \tilde{\gamma} \Omega \left(\frac{v}{v_{th}} \right)^4 (1 - \mu) \right\}$$

where $\Omega \sim (-1)$

- ▶ For each spectrum, compute $\tilde{\gamma}(n)$, μ , v/v_{th}

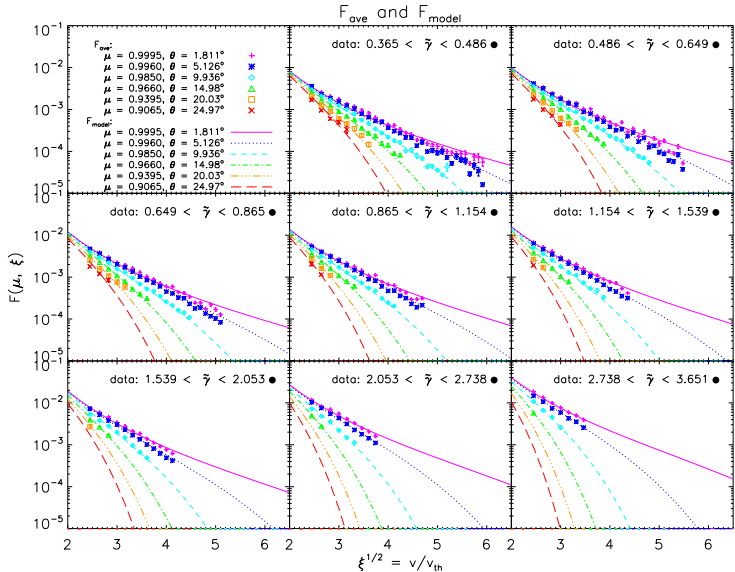


- ▶ Populate $(\mu, v/v_{th})$ -space, calculate $F_{ave} \implies$



Above: $F_{ave}(\mu, (v/v_{th})^2)$, $\tilde{\gamma} = 0.17$

F_{ave} , 2D fits (μ , (v/v_{th}))



Horaites et al., 2018a

Fit Parameters

$\tilde{\gamma} (F_{model})$	C_0	ϵ	Ω
—	model: $F(\mu, v/v_{th}) = C_0 \left(\frac{v}{v_{th}}\right)^{2\epsilon} \exp\{\tilde{\gamma}\Omega \left(\frac{v}{v_{th}}\right)^4 (1 - \mu)\}$		
$\tilde{\gamma} = 0.421$	0.157 ± 0.011	-2.13 ± 0.031	-0.38 ± 0.013
$\tilde{\gamma} = 0.562$	0.191 ± 0.014	-2.14 ± 0.033	-0.35 ± 0.013
$\tilde{\gamma} = 0.749$	0.234 ± 0.019	-2.14 ± 0.035	-0.30 ± 0.012
$\tilde{\gamma} = 1.000$	0.264 ± 0.020	-2.13 ± 0.033	-0.28 ± 0.011
$\tilde{\gamma} = 1.333$	0.306 ± 0.025	-2.13 ± 0.036	-0.27 ± 0.010
$\tilde{\gamma} = 1.778$	0.401 ± 0.040	-2.19 ± 0.045	-0.25 ± 0.011
$\tilde{\gamma} = 2.371$	0.485 ± 0.053	-2.08 ± 0.050	-0.28 ± 0.010
$\tilde{\gamma} = 3.162$	0.669 ± 0.065	-2.02 ± 0.046	-0.28 ± 0.009

Note: C_0 gives strahl amplitude, relative to the core.
Q: is this distribution stable?

Kinetic Theory and Observations of Runaway Electrons in the Solar Wind

Introduction

Kinetic Strahl Model

Observations: SWE Strahl Detector

Stability Analysis

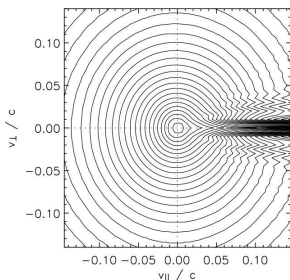
Conclusions

Anomalous Scattering of the Strahl

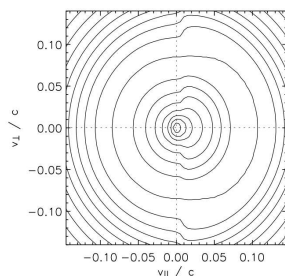
Some models propose that the strahl is scattered by wave-particle interactions.

Candidate waves:

- ▶ Whistler (e.g., Vocks et al., 2005, pictured)
- ▶ Langmuir (e.g., Seough et al., 2015)

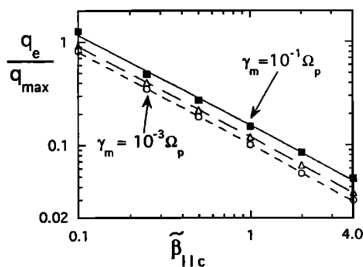


without whistlers

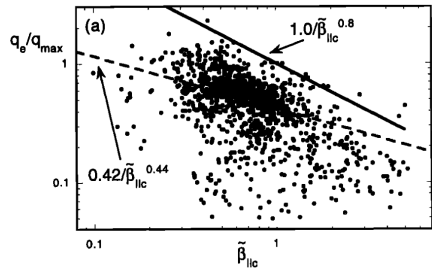


with whistlers

Whistler Heat Flux Instability



Gary et al., 1994

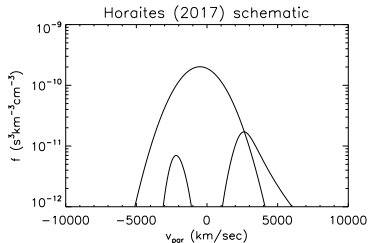
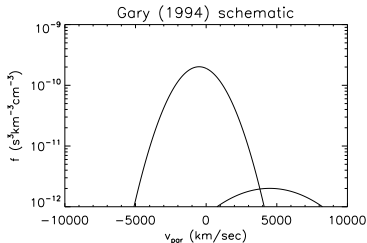


Gary et al., 1999

$$q_{\max} \sim nT v_{th}$$

Whistler Heat Flux Instability

Gary et al., (1994) proposed a model, where the electrons are described by 2 drifting Maxwellians.



Core drift v_c follows from current balance:

$$\sum_{\sigma} J_{\sigma} = 0 \rightarrow v_c = -J_s/n_c$$

How will stability analysis change if we model the strahl more realistically?

Core-strahl model (Horaites et al., 2018b)

Model distribution function as sum of core and strahl components:

$$f = f_c + f_s$$

Core distribution:

$$f_c(\mu, v) = \frac{n_c}{\pi^{3/2} v_{th}^3} \exp\left(\frac{-v^2 + 2\mu v v_c - v_c^2}{v_{th}^2}\right).$$

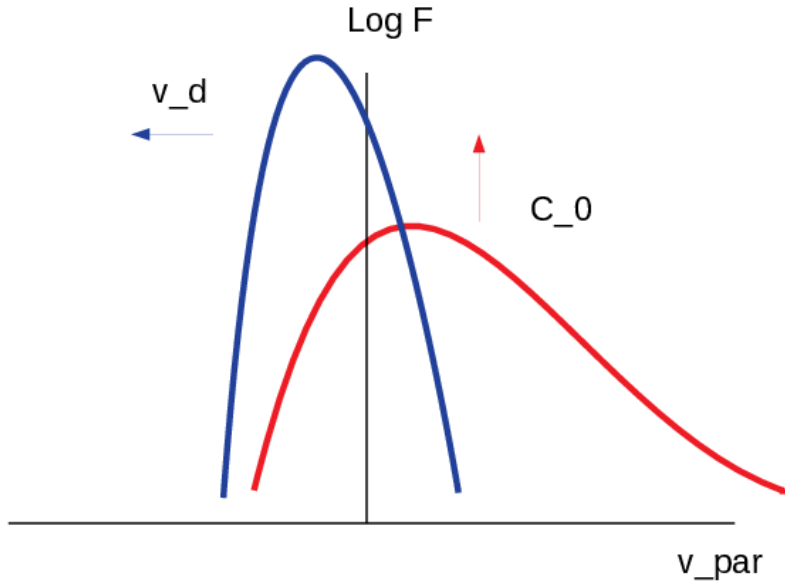
Strahl distribution:

$$f_s(\mu, v) = A(v) \frac{n_c}{v_{th}^3} C_0 \left(\frac{v}{v_{th}}\right)^{2\epsilon} \exp[\tilde{\gamma} \Omega (v/v_{th})^4 (1-\mu)],$$

where we define a truncation function $A(v)$, with $a = 10$,
 $b = 2\epsilon - 4$:

$$A(v) = \left(\frac{1}{1 + a(v/v_{th})^b}\right).$$

Require $J_{\parallel} = \int f v_{\parallel} d^3v = 0$



Dispersion Relation Solver

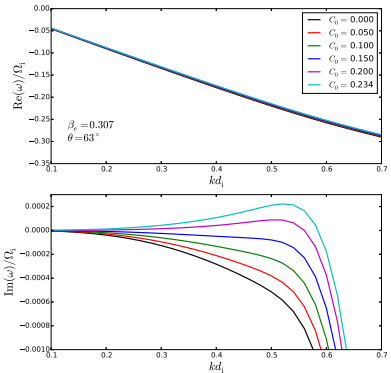
We use the kinetic dispersion relation solver, LEOPARD (Astfalk et al., 2017).

- ▶ solves kinetic equation for linear waves in magnetized plasma
- ▶ allows for arbitrary (gyrotropic) distribution functions
- ▶ can solve for modes with arbitrary propagation angle
- ▶ requires an initial guess for $\omega(\mathbf{k}) \rightarrow$ search magnetosonic, kinetic alfvén, and whistler branches

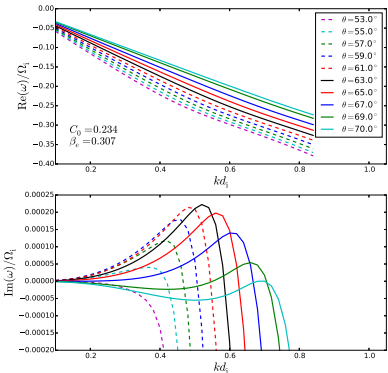
Code computes $\epsilon_{ij}(\omega, \mathbf{k})$ and solves for dispersion relation $\omega(\mathbf{k})$ from:

$$\left\{ k^2 \delta_{ij} - k_i k_j - \frac{w^2}{c^2} \epsilon_{ij}(\omega, \mathbf{k}) \right\} E_j = 0.$$

KAW Instability



$\text{Im}(\omega) \uparrow$ as $C_0 \uparrow$.

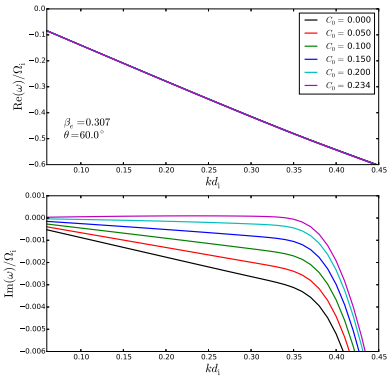


Max. growth rate at $\theta \approx 63^\circ$.

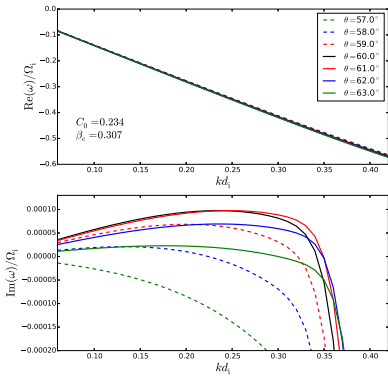
$$\Omega_i = \frac{eB}{m_p},$$

$$d_i = \frac{v_A}{\Omega_i}$$

Magnetosonic Instability



$\text{Im}(\omega) \uparrow$ as $C_0 \uparrow$.



Max. growth rate at $\theta \approx 60^\circ$.

$$\Omega_i = \frac{eB}{m_p},$$

$$d_i = \frac{v_A}{\Omega_i}$$

Resonance

Instabilities found, but which particles are affected?

Resonance condition:

$$\omega - k_{\parallel} v_{\parallel} = n \Omega_e$$

Assume $v_A \approx v_{th,i}$, and $T_i \approx T_e$ (typical conditions at 1 AU). From dispersion solver, $0.4 < kd_i < 0.6$, $0.3 \lesssim |\omega/\Omega_i| < 0.6$ Rearrange, neglecting small terms:

If $|n| > 0$,

$$|v| \approx \frac{|n| \sqrt{m_i/m_e}}{k_{\parallel} d_i} v_{th,e} \gtrsim 50 v_{th,e}$$

If $n = 0$,

$$|v| = v_A \frac{|\omega/\Omega_i|}{k_{\parallel} d_i} < v_A \ll v_{th,e}$$

Resonances do not fall in strahl regime! ($2v_{th,e} \lesssim v \lesssim 10v_{th,e}$)!

Also note for $n = 0$, resonant velocities are negative ($\omega/\Omega_i < 0$).

Isotropic halo damps growth (KAW)

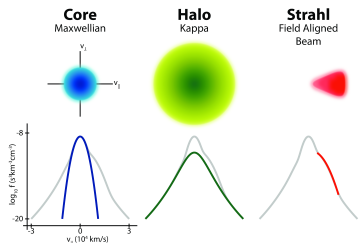
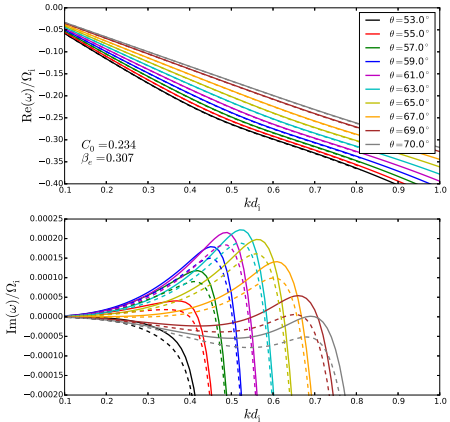
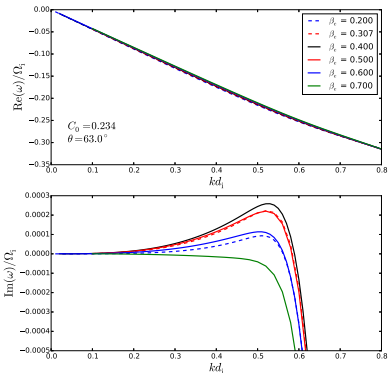


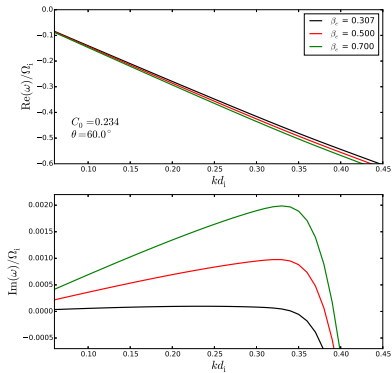
Illustration: M. Pulupa

with halo (dashed), without (solid)

Variation with β_e



KAW: as $\beta_e \uparrow$, $\text{Im}(\omega)$ reaches a maximum then stabilizes.



MS: as $\beta_e \uparrow$, $\text{Im}(\omega) \uparrow$.

β_e is smaller near the sun than at 1 AU, so MS instability may be less important at small heliocentric distances.

Kinetic Theory and Observations of Runaway Electrons in the Solar Wind

Introduction

Kinetic Strahl Model

Observations: SWE Strahl Detector

Stability Analysis

Conclusions

Conclusions

- ▶ We develop a new model of the strahl (runaway) electron population in the solar wind, which incorporates the magnetic focusing and Coulomb scattering of the distribution.
- ▶ Our model accurately describes the data at 1 AU, as measured by the Wind satellite.
- ▶ Linear analysis shows two growing modes at 1 AU: kinetic alfvén and magnetosonic. Resonate with sunward-drifting core electrons, with phase velocities $\omega/k_{\parallel} \sim v_A$.
- ▶ No whistler instability was found.

References

1. Self-Similar Theory of Thermal Conduction and Application to the Solar Wind, K. Horaites, S. Boldyrev, S. I. Krasheninnikov, C. Salem, S. D. Bale, M. Pulupa, PRL, 114 (2015) 245003
2. Kinetic Theory and Fast Wind Observations of the Electron Strahl, K. Horaites, S. Boldyrev, L. B. Wilson III, A. F. Viñas, J. Merka, MNRAS, 474 (2018), pp. 115-127
3. Stability Analysis of Core-Strahl Electron Distributions in the Solar Wind, K. Horaites, P. Astfalk, S. Boldyrev, F. Jenko, MNRAS, 480 (2018), pp. 1499-1506
4. K. Horaites, S. Boldyrev, and M. V. Medvedev, Electron strahl and halo formation in the solar wind, MNRAS, 484 (2019), pp. 24742481